

PERIODIC-COEFFICIENT FINITE-STATE AERODYNAMIC MODELING FOR ROTOR DYNAMICS OF HELICOPTER CONFIGURATIONS

R. De Troia,* M. Gennaretti† and L. Morino‡
*Dipartimento di Ingegneria Meccanica e Industriale
Università di Roma Tre, via C. Segre 60, 00146 Rome, Italy
email address: massimo@seine.dma.uniroma3.it*

Abstract

A methodology for the finite-state linear description of unsteady aerodynamic loads acting on the main rotor, when the rotor-fuselage configuration is perturbed from its equilibrium condition, is presented. In fixed-wing aircraft aerodynamics, the finite-state coefficients are time independent. For helicopter rotors this is true only for the limited case of hovering conditions with state variables describing a motion normal to the rotor disk. Otherwise, the finite-state description coefficients are time dependent and, in particular, periodic. Here, we present a methodology for the reconstruction of aerodynamic finite-state coefficients for hovering rotors subject to perturbation motion both (i) normal to the rotor disk and (ii) in the plane of the rotor disk. It is based on a boundary-element solution of the aerodynamic field induced by the Lagrangean variables of interest (for instance, amplitude of structural vibration modes, displacements of the hub, angles of rotation of the rotor disk). Under the assumptions of incompressible, potential flows, in this work, frequency-domain aerodynamic loads are determined by a boundary-element formulation for the velocity potential, coupled with the Bernoulli theorem. Numerical results for the validation of hovering rotor finite-state approximation of aerodynamic loads arising from in-plane and out-of-plane disturbances are included.

Introduction

The objective of this paper is the presentation of an efficient tool for the description of unsteady

aerodynamics loads acting on the main rotor when a hovering rotor-fuselage is perturbed from an equilibrium condition. This tool is based on: (i) a boundary-element formulation for the analysis of unsteady potential aerodynamic forces and (ii) a finite-state description of these via a matrix-fraction approximation of the aerodynamic matrix relating the vector of the aerodynamic forces to that of the Lagrangean variables. The formulation is valid for both rigid-blade and elastic-blade rotors, while the numerical results are limited to rigid-blade rotors.

The most important application of this tool is in flight dynamic, aeroelastic and aeroservoelastic modeling. In order to obtain a reliable aeroelastic analysis, an essential feature is an accurate aerodynamic load prediction. In this field, early work has dealt with two-dimensional incompressible flow configurations. In particular, for hovering rotor configurations, a methodology still widely used (in connection with a strip-theory) is that developed by Loewy [1], as an extension of the Theodorsen [2] formulation for fixed-wing analysis. The advancing-rotor configurations can also be treated in terms of lift-deficiency functions as indicated in the extended Loewy and Greenberg theories and the cascade-wake-model theory (see, e.g., Dinyavary and Friedmann [3]). Approximate methodologies based on dynamic-inflow models (extension of the momentum theory) allows for fast and reliable predictions of unsteady aerodynamic loads on rotors (see, e.g., Gaonkar and Peters [4]), even though simplified models are used for the wake effects.

Aerodynamic formulations for rotor analysis starting from the principles of conservation of mass and momentum have also been developed. In particular, a general boundary integral time-domain formulation for unsteady, compressible, potential flows for rotors has been developed in

* Research Scientist

† Assistant Professor

‡ Full Professor, AIAA Member

the past by the authors (see, e.g., Ref. [5]). Specifically, the velocity potential around a hovering rotor is determined by the corresponding boundary integral formulation; then, aerodynamic loads are evaluated through Bernoulli's theorem. The rotor aerodynamic solution is strongly influenced by the wake geometry; here, the wake geometry is assumed to be prescribed with the shape given either by the generalized wake model introduced by Landgrebe [6], or by the simple helicoidal-surface function.

A linear finite-state aerodynamics modeling is an approximation of the aerodynamic operator around a given reference configuration, which allows one to recast the dynamics equation in state-space format. The most common approaches used in the literature for fixed-wings are those introduced by Roger [7] and Karpel [8]. More recently a least-square fraction-matrix approximation technique was introduced by Ghiringhelli and Mantegazza [9] (see also Morino et al. [10]), to which the reader is referred for a review of the state of the art.

Indeed, for aircraft dynamic analysis, it is desirable to have an approximation of the aerodynamic forces in a finite-state format in order to express the dynamics of the system considered (aerodynamic forces included) in standard state-space form. Note that such representation is useful for the stability analysis and is essential for the design of control laws.

Next consider hovering-rotor configurations. If the perturbation motion is normal to the rotor disk the basic methodology of Refs. [9] and [10] is still applicable. However, in this case, a large number of augmented states is required, due to the complexity of the wake geometry. Venkatesan and Friedmann [11] developed the finite-state approximation of the Loewy's deficiency function based on the Bode-plot approach, together with a least square procedure. A new finite-state formulation has been introduced by Peters and Cao [12] and Peters and He [13] for the description of the wake-induced velocity over the rotor disk. This approach is based on an induced-flow expansion of the induced flow derived directly from the potential-flow formulation (the coefficients of the expansion are the aerodynamic states). According to Refs. [12] and [13], the advantages of this formulation are: (i) no numerical fitting of frequency-response or indicial functions is needed; (ii) few states are needed for a

convenient aerodynamic approximation; (iii) the resulting equations are easily coupled with structural or control equations. The limitations are: (i) the rotor is assumed to be a thin, undeformed disk; (ii) only normal-disk loads can be described; (iii) only cylindrical wakes are implemented. This methodology is applicable also to forward flight case.

In the present work, the finite-state approximation of Refs. [9] and [10] (in connection to the boundary-element approach mentioned above) is extended to the case of rotors. In particular, in addition to the case of hovering blades with perturbation motion normal to the rotor disk (time-independent-coefficient finite-state model), the case of hovering blades with in-plane perturbations (periodic-coefficient finite-state model) is considered. Numerical results are presented in order to assess the finite-state approximation used here for both fixed-wing and rotary-wing configurations.

The theoretical formulation was developed jointly by the three authors. The implementation and the numerical results are obtained by De Troia, as part of his doctoral work [14].

Aerodynamic Formulation

The aerodynamic formulation is based on the assumptions of incompressible, quasi-potential flows. These are flows that are potential everywhere in the field except for the wake points (see, e.g., Ref. [5] for details of this section). Thus, if \mathbf{v} denotes the velocity of the fluid particles, it is possible to introduce the potential function φ such that $\mathbf{v} = \nabla\varphi$, for $\mathbf{x} \in \mathcal{V} \setminus \mathcal{S}_w$, where \mathcal{V} denotes the fluid region, and \mathcal{S}_w denotes the wake surface. Combining the above equation with continuity equation, $\nabla \cdot \mathbf{v} = 0$, one obtains the following Laplace equation

$$\nabla^2 \varphi = 0 \quad \text{for } \mathbf{x} \in \mathcal{V} \setminus \mathcal{S}_w. \quad (1)$$

The formulation is presented for a frame of reference connected to the undisturbed air. Thus, we have $\varphi = 0$ at infinity. In addition, we need boundary conditions on body and wake. The body is assumed to be impermeable, and accordingly the boundary condition on the body surface, \mathcal{S}_B , is $(\mathbf{v} - \mathbf{v}_B) \cdot \mathbf{n} = 0$, where \mathbf{v}_B is the velocity of the points of \mathcal{S}_B , and \mathbf{n} is the unit normal to

S_B . Recalling that $\mathbf{v} = \nabla\varphi$, one obtains

$$\frac{\partial\varphi}{\partial n} = \mathbf{v}_B \cdot \mathbf{n} \quad \text{for } \mathbf{x} \in S_B. \quad (2)$$

Boundary conditions on the wake are obtained from the principles of conservation of mass and momentum across a surface of discontinuity, such as S_w . These yield $\mathbf{v} \cdot \mathbf{n} = \mathbf{v}_w \cdot \mathbf{n}$ and $\Delta p = 0$. In turn, in terms of velocity potential φ , these yield

$$\Delta \left(\frac{\partial\varphi}{\partial n} \right) = 0 \quad (3)$$

on the wake surface, and

$$\Delta\varphi = \text{constant} \quad (4)$$

following a wake material point. At the trailing edge we impose that $\Delta\varphi$ on the body equals $\Delta\varphi$ on the wake.

Starting from this differential formulation, applying the boundary-integral-equation technique, and using Eq. (3), the potential-flow solution for a lifting body satisfies the following equation:

$$\begin{aligned} \varphi(\mathbf{x}) = & \int_{S_B} \left(\frac{\partial\varphi}{\partial n} G - \varphi \frac{\partial G}{\partial n} \right) dS(\mathbf{y}) \\ & - \int_{S_w} \Delta\varphi \frac{\partial G}{\partial n} dS(\mathbf{y}), \end{aligned} \quad (5)$$

where G is the unit source $G = -1/4\pi||\mathbf{y} - \mathbf{x}||$. Equation (5) is an integral representation of φ in the field in terms of φ and $\partial\varphi/\partial n$ on S_B and $\Delta\varphi$ on S_w . If \mathbf{x} tends to the surface S_B , we obtain, in the limits, an integral compatibility relationship between φ and $\partial\varphi/\partial n$ on S_B , and $\Delta\varphi$ on S_w . In our case $\partial\varphi/\partial n$ on S_B is known from Eq. (2) and $\Delta\varphi$ from the preceding time history (see Eq. (4)); hence the compatibility relationship corresponds to a boundary integral equation for φ on S_B . Once φ on S_B has been obtained, the application of the unsteady Bernoulli theorem gives the pressure distribution over the body surface, and hence the aerodynamic loads acting on the body. The boundary element method used here consists of a zeroth-order (i.e., piecewise constant) discretization of the above integral formulation.

Finite-State Modeling for Rotary Wings

with Blade-Frame Fixed Perturbations

For hovering rotor configurations, where the wake surface is assumed to be fixed with respect to

the body, it is possible to recast Eq. (5) in the frequency-domain. Then, using the linearized Bernoulli theorem and under the assumption of blade perturbation motion (like, e.g., flapping, pitching and lagging) or rotor disk (fuselage) out-of-plane perturbation motion (like, e.g., linear velocity aligned with the rotor axis) one obtains a linear relationship between the set of state variables defining such body motion (and thereby the body boundary condition for φ , see Eq. (2)) and the consequent generalized aerodynamic forces acting on the body. This may be recast in terms of the so-called aerodynamic transfer matrix, as discussed below.

Aerodynamic Matrix

The aerodynamic matrix, \mathbf{E} , which in the frequency domain relates the dimensionless vector of the state variables, $\bar{\mathbf{q}} = \{\bar{q}_i\}$ (where q_i are the dimensionless Lagrangean variables of the blade motion), to the vector of the generalized aerodynamic forces, $\bar{\mathbf{e}}$, is obtained by the product of a set of frequency-dependent matrices. Specifically, we have

$$\bar{\mathbf{e}} = q_D \mathbf{E}(\bar{s}) \bar{\mathbf{q}} = q_D \mathbf{E}_4 \mathbf{E}_3(\bar{s}) \mathbf{E}_2(\bar{s}) \mathbf{E}_1(\bar{s}) \bar{\mathbf{q}} \quad (6)$$

where $q_D = \rho\Omega^2 R^2/2$ is the reference dynamic pressure (denoting with Ω the angular velocity of the rotor) and ρ the density of the air, whereas $\bar{s} = s/\Omega$ is the reduced Laplace-transform variable. In addition, $\mathbf{E}_1(\bar{s})$ gives the normal-wash, $\bar{\chi} = \partial\bar{\varphi}/\partial n$, in terms of the state variables, $\mathbf{E}_2(\bar{s})$ corresponds to the above mentioned discretization of the operator in Eq. (5), $\mathbf{E}_3(\bar{s})$ relates the pressure distribution with the values of the potential on the body surface (unsteady linearized Bernoulli theorem), and finally \mathbf{E}_4 yields the generalized aerodynamic forces from the pressure distribution.

The expressions of the matrices involved in Eq. (6) have been presented in [15] for the fixed-wing case, and extended in [16] to fixed-axis rotors in uniform rotation.

In Figs. 1 and 2, we present the comparison between load prediction from the boundary-element methodology described and from Loewy's theory [1]. In these figures real and imaginary parts of the flapping moment coefficient due to a unit flapping-mode displacement, $M_{\beta\beta}$, for a rotor wake with pitch $h = 0.5c$, where c denotes the chord length are illustrated (in all the

figures $k = \Im m[\bar{s}]$. The results obtained with the BEM formulation presented have been computed by assuming a simple helicoidal wake geometry. For the wake pitch considered, our results and those from the Loewy's approach agree quite well (however, the agreement deteriorates as the wake pitch increases as expected, given the assumptions of Loewy [1] on the wake vorticity spatial distribution). Other terms of the aerodynamic matrix have the same behavior.

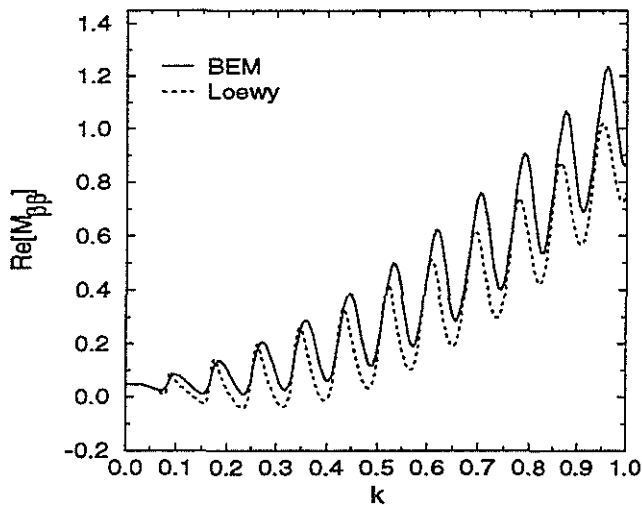


Figure 1. $M_{\beta\beta}$ vs k for $h/c = 0.5$. Present results: BEM and Loewy/strip-theory method.

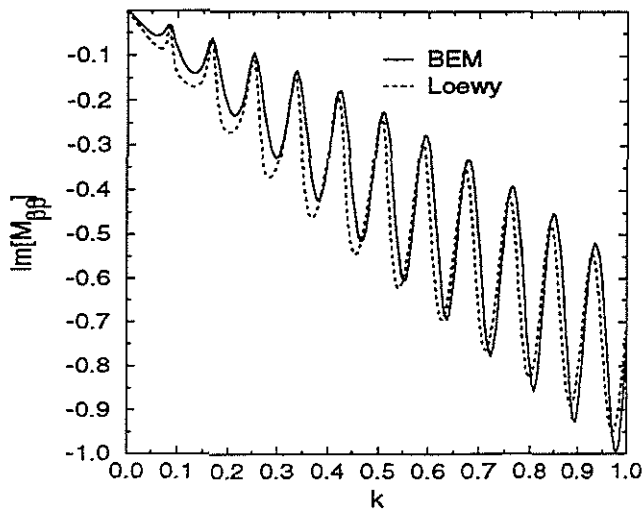


Figure 2. $M_{\beta\beta}$ vs k for $h/c = 0.5$. Present results: BEM and Loewy/strip-theory method.

Constant-Coefficient Finite-State Modeling

From the expression of the boundary-element formulation in frequency-domain used for the potential-flow solution, it is possible to observe that the elements of the matrix $\mathbf{E}(\bar{s})$ are typically transcendental functions of the reduced Laplace-variable \bar{s} . Hence, the transfer matrix is relatively easy to use in problems regarding the identification of instability margins (e.g., $V-g$ plots), but not in dynamic-response problems or for designing a control device. In order to overcome these limits of applicability, it is convenient to determine a finite-state model for the aerodynamic operator.

Here, following the procedure introduced in [9] (see also [10]), we take advantage of the fact that, for high-frequencies and displacement state variables, the leading term is of order \bar{s}^2 (stemming from the derivative that appears in the boundary condition and in Bernoulli's theorem). Thus, we choose a finite-state model for the hovering rotor aerodynamic matrix given by a matrix-fraction approximation of the type

$$\mathbf{E}(\bar{s}) \approx \hat{\mathbf{E}}(\bar{s}) = \bar{s}^2 \mathbf{A}_2 + \bar{s} \mathbf{A}_1 + \mathbf{A}_0 + \left(\sum_{i=0}^N \mathbf{D}_i \bar{s}^i \right)^{-1} \left(\sum_{i=0}^{N-1} \mathbf{R}_i \bar{s}^i \right). \quad (7)$$

The matrices \mathbf{A}_i , \mathbf{D}_i and \mathbf{R}_i are real and fully populated (except for \mathbf{D}_N that coincides with the identity matrix) and are determined by a least-square approximation technique. This consists of setting

$$\epsilon^2 = \sum_n w_n \text{Tr} [\mathbf{Z}^*(jk_n) \mathbf{Z}(jk_n)] = \min, \quad (8)$$

where $k = \Im m[\bar{s}]$, whereas w_n denote suitable weights, and

$$\mathbf{Z}(\bar{s}) := \left(\sum_{n=0}^N \mathbf{D}_n \bar{s}^n \right) [\bar{s}^2 \mathbf{A}_2 + \bar{s} \mathbf{A}_1 + \mathbf{A}_0 - \mathbf{E}(\bar{s})] + \sum_{n=0}^{N-1} \mathbf{R}_n \bar{s}^n \quad (9)$$

is a weighted measure of the error $(\mathbf{E} - \hat{\mathbf{E}})$. In order to apply the matrix-fraction approximation of the aerodynamic matrix and derive the time-domain relationship between the generalized forces, \mathbf{e} , and the state variables, \mathbf{q} , it is possible

and convenient to recast Eq. (7) in the following form

$$\hat{\mathbf{E}}(\hat{s}) = \hat{s}^2 \mathbf{A}_2 + \hat{s} \mathbf{A}_1 + \mathbf{A}_0 + \mathbf{H}(\hat{s}\mathbf{I} - \mathbf{G})^{-1} \mathbf{F} \quad (10)$$

where \mathbf{H} depends upon the \mathbf{R}_i 's, \mathbf{G} upon the \mathbf{D}_i 's, whereas $\mathbf{F}^T = [\mathbf{I}, \mathbf{0}, \dots, \mathbf{0}]$ (see [9] or [10] for details).

Note that the accuracy of the approximation depends upon the number, N , of matrices used in the matrix-fraction term in Eq. (7). The appropriate value of N depends upon the characteristics of the functions to be approximated. In our case, these functions corresponds to the elements of the matrix \mathbf{E} in terms of the frequency and, for the problem of an hovering rotor, they show a wavy behavior (see, e.g., Figure 1), which requires a high value of N . This, in turn, may induce an instability (i.e., real part greater than zero) in some of the eigenvalues of the matrix \mathbf{G} in Eq. (10); these are spurious poles which are introduced by the interpolation procedure. In order to overcome this problem the iterative procedure of Ref. [9] is adopted. This consists of: (i) diagonalization (or block-diagonalization) of \mathbf{G} , (ii) truncation of the unstable states (the matrix \mathbf{G} is modified into a smaller matrix $\hat{\mathbf{G}}$), and (iii) application of an optimal fit iterative procedure to determine new matrices $\hat{\mathbf{A}}_2, \hat{\mathbf{A}}_1, \hat{\mathbf{A}}_0, \hat{\mathbf{F}}$, and $\hat{\mathbf{H}}$ that replace, respectively, $\mathbf{A}_2, \mathbf{A}_1, \mathbf{A}_0, \mathbf{F}$, and \mathbf{H} (whereas $\hat{\mathbf{G}}$ remains unchanged throughout the iteration). Hence, the matrix-fraction finite-state approximation assuring a good and stable fit of $\mathbf{E}(\hat{s})$ has the final form

$$\hat{\mathbf{E}}(\hat{s}) = \hat{s}^2 \hat{\mathbf{A}}_2 + \hat{s} \hat{\mathbf{A}}_1 + \hat{\mathbf{A}}_0 + \hat{\mathbf{H}}(\hat{s}\mathbf{I} - \hat{\mathbf{G}})^{-1} \hat{\mathbf{F}}. \quad (11)$$

Then, from Eq. (11) it is possible to derive the time-domain expression of generalized forces in terms of the state variables, which is given by the following set of constant-coefficient linear differential relations

$$\mathbf{e} = q_D(\ddot{\mathbf{A}}_2 \mathbf{q} + \ddot{\mathbf{A}}_1 \dot{\mathbf{q}} + \ddot{\mathbf{A}}_0 \mathbf{q} + \ddot{\mathbf{H}} \mathbf{r}) \quad (12)$$

$$\dot{\mathbf{r}} = \ddot{\mathbf{G}} \mathbf{r} + \ddot{\mathbf{F}} \mathbf{q}, \quad (13)$$

where \mathbf{r} is the vector of the augmented-state variables, introduced by the finite-state approximation, and (\cdot) denotes differentiation with respect to the dimensionless time variable $\hat{t} = \Omega t$.

In conclusion, Eq. (11) allows for a uniformly valid frequency-domain expression for the generalized aerodynamic matrix and hence for the

transfer function of the dynamic system. This methodology is strictly valid for the case of wings and hovering rotors with blade perturbation motion and/or out-of-plane disk (fuselage) perturbation motion. In the following we extend the formulation at the case of hovering rotors with in-plane disk (fuselage) perturbation motion.

Finite-State Modeling for Rotary Wings

with Fuselage-Frame Fixed Perturbations

For hovering rotors with perturbation motion in the plane of disk it is not possible to express the aerodynamic operator in the frequency domain. This is due to the presence of additional periodic terms, of rotational frequency Ω , in the impermeability boundary conditions induced by change of orientation of the blades with respect to the perturbation velocity during one revolution. Additional periodic terms in the aerodynamic operator also arise in the expression of generalized forces if these are referred to the in-plane modes of the whole rotor. Indeed, denoting with \mathbf{e} the vector of generalized aerodynamic forces acting on a rigid blade expressed in the blade frame, and with \mathbf{f} the vector of the same forces expressed in the air frame¹, the two are related by

$$\mathbf{f} = \begin{bmatrix} \cos \Omega t & \sin \Omega t & 0 & 0 & 0 & 0 \\ \sin \Omega t & -\cos \Omega t & 0 & 0 & 0 & 0 \\ 0 & 0 & 1 & 0 & 0 & 0 \\ 0 & 0 & 0 & \cos \Omega t & \sin \Omega t & 0 \\ 0 & 0 & 0 & \sin \Omega t & -\cos \Omega t & 0 \\ 0 & 0 & 0 & 0 & 0 & 1 \end{bmatrix} \mathbf{e} \quad (14)$$

Note that this periodicity would also arise in the case of blade-frame fixed disturbances discussed in the preceding section. Nevertheless, in that case the finite-state modeling described in the preceding section may be applied for the vector \mathbf{e} , and then the periodic finite-state modeling is determined by Eq. (14).

On the other hand, a different finite-state modeling technique has to be applied in order to take into account the periodicity induced by the body boundary conditions. Denoting with u and v the in-plane components of the linear perturbation velocity of the rotor disk (or fuselage center of

¹ The first (last) three components of \mathbf{e} and \mathbf{f} are the physical components of force (moment); the third component of force (moment) is in the direction normal to the rotor disk plane.

mass), and with p and q the in-plane components of the angular perturbation velocity of the rotor disk (or fuselage) in the same frame, we have

$$\begin{aligned} \mathbf{v}'_B = & (u \cos \Omega t + v \sin \Omega t) \mathbf{i}_B \\ & + (u \sin \Omega t - v \cos \Omega t) \mathbf{j}_B \\ & + (q \cos \Omega t - p \sin \Omega t) z \mathbf{i}_B \\ & + (p \cos \Omega t + q \sin \Omega t) z \mathbf{j}_B \\ & + p(\sin \Omega t - q \cos \Omega t) x \mathbf{k}_B \\ & - p(\cos \Omega t + q \sin \Omega t) y \mathbf{k}_B \end{aligned} \quad (15)$$

where x , y and z are the Cartesian coordinates of position vector in the blade frame with base unit vectors $\mathbf{i}_B, \mathbf{j}_B$ and \mathbf{k}_B . Combining Eq. (15) with Eq. (2) one obtains the following perturbation boundary conditions

$$\chi(\mathbf{x}, t) = \mathbf{v}'_B \cdot \mathbf{n} = \sum_i \psi_i(\mathbf{x}, t) q_i(t)$$

where $\psi_i(\mathbf{x}, t) = \tilde{\psi}_i(\mathbf{x}) \exp^{j\Omega t} + \text{c.c.}$ Setting $q_i(t) = \tilde{q}_i \exp^{j\omega t} + \text{c.c.}$, we have

$$\begin{aligned} \chi(\mathbf{x}, t) = & \tilde{\chi}^0(\mathbf{x}) \exp^{j\omega t} + \tilde{\chi}^+(\mathbf{x}) \exp^{j(\Omega+\omega)t} \\ & + \tilde{\chi}^-(\mathbf{x}) \exp^{j(\Omega-\omega)t} + \text{c.c.} \end{aligned}$$

(for details see [14]). From $\tilde{\chi}^0, \tilde{\chi}^+$ and $\tilde{\chi}^-$, one can determine three different aerodynamic matrices of the type of that of Eq. (6), and then three different finite-state models of the type of that expressed by Eqs. (12) and (13). Finally, combining these approximations as specified in Eq. (16), one obtains the time-domain finite-state model

$$\dot{\mathbf{e}}(t) = \mathbf{A}_1(t) \dot{\mathbf{q}} + \mathbf{A}_0(t) \mathbf{q} + \mathbf{H} \mathbf{r} \quad (16)$$

$$\dot{\mathbf{r}} = \mathbf{G} \mathbf{r} + \mathbf{F}(t) \mathbf{q} \quad (17)$$

where the matrices \mathbf{A}_1 , \mathbf{A}_0 and \mathbf{F} are periodic function of time; on the other hand, the matrices \mathbf{H} and \mathbf{G} are time independent (see [14] for details).

Numerical Results

First, we have accomplished a finite-state approximation for the aerodynamic generalized forces in the case of time-independent operator. In this case, we have considered a two-bladed rotor with collective pitch angle $\theta_0 = 8^\circ$, and a helicoidal wake geometry. First, in the matrix-fraction approximation we considered a number of poles $N_p = 26$ (number of eigenvalues of the

matrix \mathbf{G} in Eq. (10)). Using this number of poles, the least-square procedure gave some unstable poles which induces considerable local inaccuracy in the approximation of the aerodynamic matrix, in the range from $k = 0$ to $k = 1$. Then, eliminating these unstable poles, and re-evaluating some of the matrices in the approximated expression we obtain a very good agreement between the calculated and the approximated aerodynamic forces, as shown in Figs. 3 and 4 for the $M_{\beta\beta}$ coefficient (the final number of stable poles is $N_p = 19$). Note that, if a good accuracy of

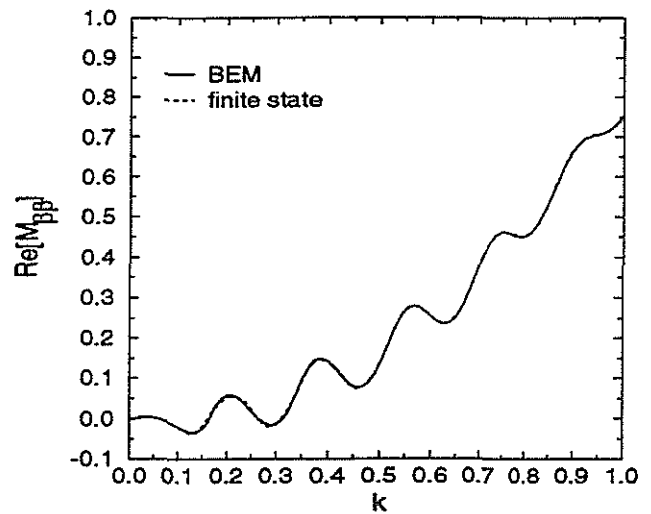


Figure 3. Real part of $M_{\beta\beta}$ vs k for $\theta_0 = 8^\circ$. BEM results (helicoidal wake) and their finite-state approximation ($N_p = 19$).

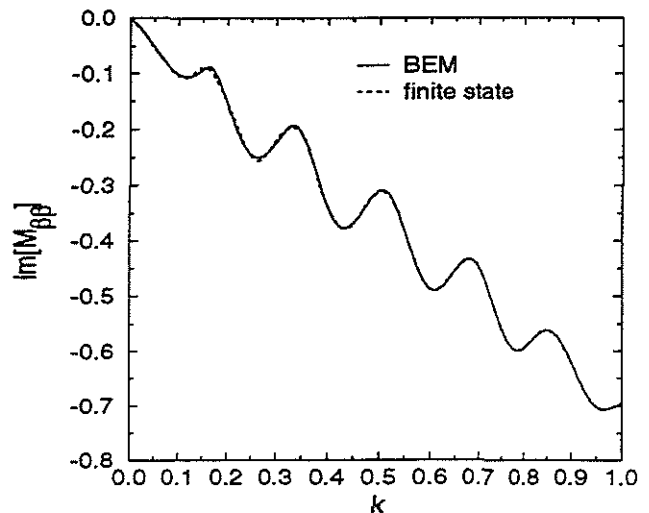


Figure 4. Imaginary part of $M_{\beta\beta}$ vs k for $\theta_0 = 8^\circ$. BEM results (helicoidal wake) and their finite-state approximation ($N_p = 19$).

the approximation is desired only in the low frequency range, then a lower number of poles may be used (see Ref. [16]). Indeed, in order to have an accurate approximation of $\text{Re}(M_{\beta\beta})$ in the range from $k = 0$ to $k = 0.5$, only 14 poles are needed (see Fig. 5). Note also that for $k > 0.5$, although the accuracy decreases, the overall behavior of the curve is well captured.

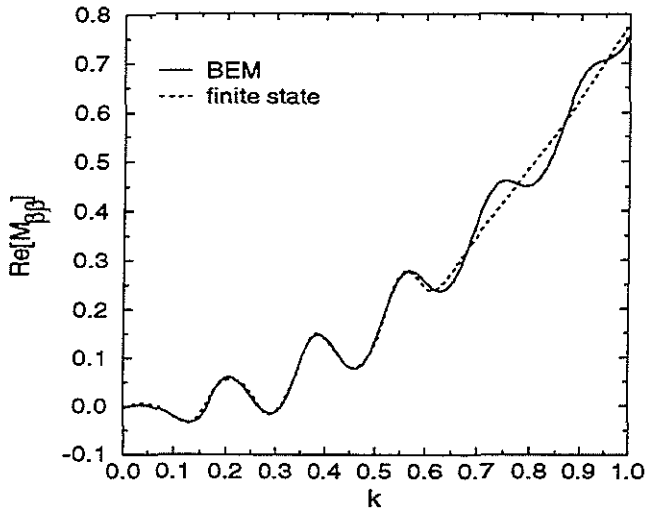


Figure 5. Real part of $M_{\beta\beta}$ vs k for $\theta_0 = 8^\circ$. BEM results (helicoidal wake) and their finite-state approximation ($N_p = 14$).

Next, we consider the finite-state approximation for periodic-coefficient operator; numerical results are obtained for a single-bladed rotor with collective pitch angle $\theta_0 = 5^\circ$ and helicoidal wake geometry, perturbed by an horizontal velocity in air frame. Results obtained by using the time-domain boundary integral formulation presented above are compared with those from periodic-coefficient finite-state model extracted from the BEM results. Figures (6) and (7) present time histories of dimensionless horizontal and vertical forces (made dimensionless using $\frac{1}{2}\rho\Omega^2 R^2$) in blade-frame, in presence of an horizontal harmonic gust (with reduced frequency $k = 0.1$). We note a good agreement between direct time-domain method and periodic-coefficient finite-state model, as one can see in Figs. (8) and (9) (a stretching of previous Figs. (6) and (7)).

Concluding Remarks

A boundary-element approach for time- and frequency-domain analysis of hovering rotor aerodynamics has been presented with a finite-

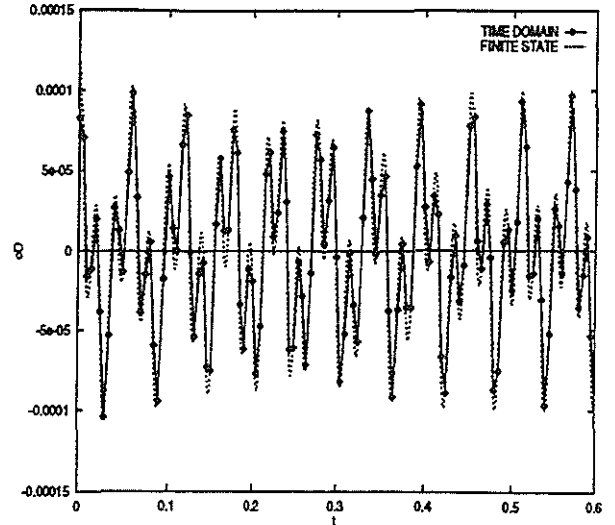


Figure 6. Nondimensional horizontal force due to horizontal disturbance. Comparison between direct time-marching BEM solution and periodic-coefficient finite-state model.

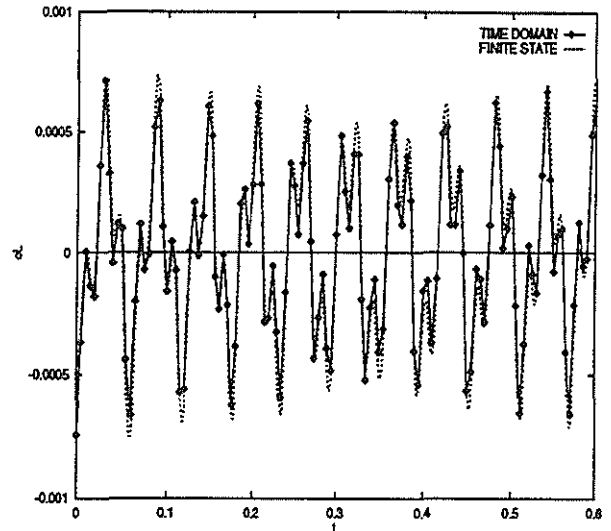


Figure 7. Nondimensional vertical force due to horizontal disturbance. Comparison between direct time-marching BEM solution and periodic-coefficient finite-state model.

state model for the aerodynamic matrix based on a matrix-fraction approximation. Both time-independent coefficient models (typical of fixed wings and of hovering rotors with blade-motion perturbations) and periodic-coefficient models (related to hovering blades with air-frame perturbations in the rotor disk plane) are presented. By coupling finite-state aerodynamics with the equations of system dynamics, it is possible to recast the complete system in state-space format, which is computationally more convenient. Numerical results that validate the aerodynamic solution as well as the finite-state mod-

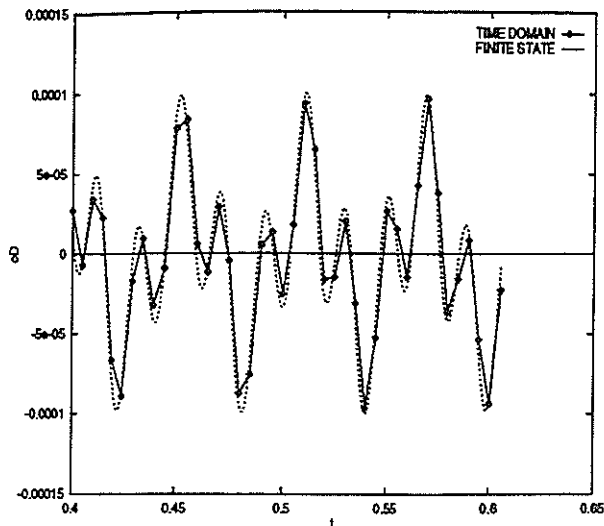


Figure 8. Nondimensional horizontal force due to horizontal disturbance. Comparison between direct time-marching BEM solution and periodic-coefficient finite-state model.

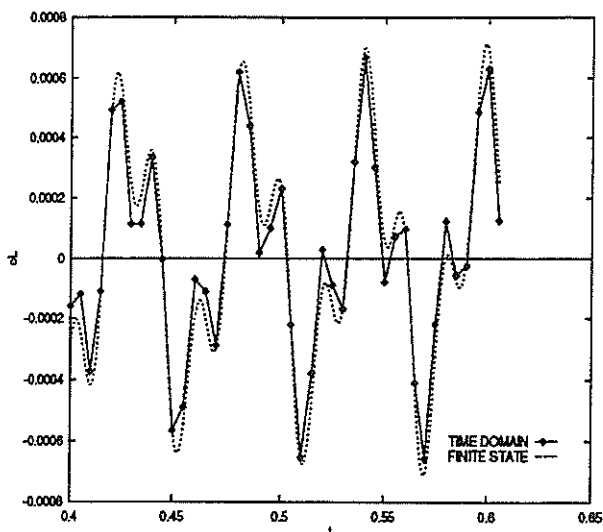


Figure 9. Nondimensional vertical force due to horizontal disturbance. Comparison between direct time-marching BEM solution and periodic-coefficient finite-state model.

el have been presented. The finite-state model results have shown the capability of very accurate approximations of the numerical solutions by introducing a certain number of poles (i.e., additional aerodynamic states). It has been shown also that the number of poles may be modified according to the frequency range in which higher accuracy is required. For periodic-coefficient hovering rotor the accuracy of the finite-state model introduced is quite good.

Finally, note that in Eq. (16) the matrix \mathbf{G} represents the dynamics of the augmented states. Hence the fact that \mathbf{G} is time independent is in

agreement with the hovering rotor model used since the augmented states take into account the wake effects on aerodynamic field. Indeed, in general, these effects depend on the wake shape and on the vorticity distribution which in turn depends on the state variables: therefore, in our case the effect of state variables on the augmented states is expressed by the matrix \mathbf{F} , whereas the effect of the wake shape is expressed by the time-independent matrix \mathbf{G} .

For advancing rotors this is not true, the wake moves in the body frame and hence also the matrix \mathbf{G} is periodic in the differential equation for the augmented states.

It is easy to see that the finite-state periodic-coefficient model of Eq. (16) is valid also for elastic state variable case; this case is discussed in Ref. [14].

References

1. Loewy, R.G., "A Two-Dimensional Approximation of Unsteady Aerodynamics of Rotary Wings," *Journal of Aeronautical Sciences*, Vol. 24, No. 2, 1957, pp. 81-92.
2. Theodorsen, T., "General Theory of Aerodynamic Instability and the Mechanism of Flutter," NACA TR 496, 1949.
3. Dinyavari, M.A.H., and Friedmann, P., "Unsteady Aerodynamics in Time and Frequency Domains for Finite Time Arbitrary Motion of Rotary Wings in Hover and Forward Flight," AIAA Paper 84-0988, 1988.
4. Gaonkar, G.H., and Peters, D.A., "Review of Dynamic Inflow Modeling for Rotorcraft Flight Dynamics," *Vertica*, Vol. 12, No. 3, 1988, pp. 213-242.
5. Morino, L., and Gennaretti, M., "Boundary Integral Equation Methods for Aerodynamics," *Computational Nonlinear Mechanics in Aerospace Engineering, AIAA Progress in Aeronautics and Astronautics - 146*, edited by S.N. Atluri, AIAA, Washington, DC, 1992, pp. 279-321.
6. Landgrebe, A.J., "An Analytical and Experimental Investigation of Helicopter Rotor Hover Performance and Wake Geometry Characteristics," USAAMRDL TR 71-24, 1971.
7. Roger, K.L., "Airplane Math Modeling Methods for Active Control Design," AGARD-CP 228, 1977.
8. Karpel, M., "Design for the Active Flutter Suppression and Gust Alleviation Using State-Space Aeroelastic Modeling," *Journal of Aircraft*, Vol. 19, 1982, pp. 221-227.
9. Ghiringhelli, G.L., and Mantegazza, P., "Interpolation Extrapolation and Modeling of Unsteady Linear(ized) Aerodynamic Forces," *Proceedings of the International Forum on Aeroelasticity and Structural Dynamics*, AAAF, Strasbourg, France, 1993, pp. 207-221.
10. Morino, L., Mastroddi, F., De Troia, R., Ghiringhelli, G.L., and Mantegazza, P., "Matrix Fraction

- Approach for Finite-State Aerodynamic Modeling," *AIAA Journal*, Vol. 33, No. 4, 1995, pp. 703-711.
11. Venkatesan, C., and Friedmann, P.P., "New Approach to Finite-State Modeling of Unsteady Aerodynamics," *AIAA Journal*, Vol 24, No. 12, 1986, pp. 1889-1897.
 12. Peters, D.A., Cao, W.M., "Finite State Induced Flow Models. Part I: Two-Dimensional Thin airfoil," *Journal of Aircraft*, Vol. 32, No. 5, pp. 313-322, 1995.
 13. Peters, D.A., He, C.J., "Finite State Induced Flow Models. Part II: Three-Dimensional Rotor Disk," *Journal of Aircraft*, Vol. 32, No. 5, pp. 323-333, 1995.
 14. De Troia, R., *Modellazione agli Stati Finiti di Operatori Aerodinamici in Presenza di Controlli*, Doctoral Dissertation, Università di Roma 'La Sapienza', Roma, Italy, 1997 (in Italian).
 15. Morino, L., "Steady, Oscillatory, and Unsteady Subsonic and Supersonic Aerodynamics - Production Version (SOUSSA - P 1.1) - Volume I - Theoretical Manual," NASA CR 159130, 1980.
 16. Gennaretti, M., Cicalé, M., Mastroddi, F., and Morino, L., "Aerodynamic Modeling for Hovering Rotor Dynamic Response and Aeroelasticity," Sixth Int'l Workshop on Dynamics and Aeroelastic Stability Modeling of Rotorcraft Systems, Los Angeles, CA, 1995.

Acknowledgements

The authors wish to acknowledge the contribution of Dr. Marco Cicalè who was involved in the initial stage of the work.